Philippine Journal of Science
154 No. 1: 207-216, February 2025
ISSN 0031 - 7683
Date Received: 17 July 2024

Contraction of a Wave Packet while Scattering with a Step Potential

Vincent Gene L. Otero and Anthony Allan D. Villanueva*

Institute of Physics, University of the Philippines Los Baños,
College, Los Baños, Laguna 4031 the Philippines

A free particle represented by a Gaussian wave packet with a negative statistical correlation between the position and momentum can have a decreasing position uncertainty (or wave packet contraction) for a finite duration. We numerically simulate particle scattering in such a Gaussian state with a step potential barrier to see if the contraction is still present. The time-dependent Schrödinger equation (TDSE) was solved using the Crank-Nicolson method implemented in the Python programming language. We show that with a negative position-momentum correlation, the incident Gaussian wave packet and the reflected wave packet both exhibit a persistent contractive behavior. This particle localization suggests that more precise position measurements during barrier scattering events beyond the standard quantum limit are possible.

Keywords: Crank-Nicolson, position-momentum covariance, position uncertainty, quantum mechanics, step potential

INTRODUCTION

In quantum mechanics, the wave property of a microscopic particle (10^{-9} m or smaller) manifests when it encounters a potential barrier. Mathematically, the particle is modeled as a wave packet in position-space. This assumes that the particle momentum is no longer definite. Instead, there is a spread of momenta of order Δp (the momentum uncertainty) representing the coherent superposition of different momentum states. The dispersion and propagation of this wave packet are determined by the time-dependent Schrödinger equation (TDSE). Simulations such as the seminal paper of Goldberg, Schwarz, and Schey (Goldberg *et al.* 1967) have shown that the particle's wave packet in position-space typically breaks up into two wave groups – a reflected wave group and a transmitted wave group – which is dependent on the relationship between the incident kinetic energy E and barrier height V_0. This splitting represents the superposition of the "reflected' and "transmitted" states – an analog of the celebrated Schrödinger cat state in being a superposition of "alive" and "dead" states. Such models possess a more detailed and vivid description of quantum scattering off a barrier than the stationary plane wave analysis using the time-independent Schrödinger equation or TISE (Smith and Blaylock 2017; van Dijk *et al.* 2020).

A free particle represented by a Gaussian wave packet in position space with a negative statistical correlation between its position and momentum can have, under certain circumstances, a decreasing position uncertainty *i.e.* wave packet contraction (Yuen 1983; Robinett *et al.* 2005; Tannor 2007; Villanueva 2018). This means the particle's position uncertainty Δx is not larger than the initial position uncertainty $(\Delta x)_0$ within a certain finite duration Δt since the wave packet contraction is only temporary. Recall that the position uncertainty Δx is a fundamental limit set by quantum mechanics itself on the "resolving power" of the particle detector, *i.e.* the particle cannot be located with an accuracy finer than Δx. Position measurements performed within Δt will, therefore, be more accurate compared to measurements using the minimum uncertainty wave packet.

*Corresponding author: advillanueva1@up.edu.ph

Prior to this study, it was unknown if wave packet contraction would still manifest if the Gaussian wave packet scatters off a step barrier potential. A numerical scheme that solves the TDSE for any reasonable initial wave function and potential is an essential tool for investigating this hypothesis. The Crank-Nicolson (C-N) method is an unconditionally stable numerical scheme that propagates the wave packet over time in a unitary manner (Press *et al.* 1986; Landau, Paez, and Bordeianu 2015). In this paper, the authors prepared using the C-N method a numerical simulation of the time-dependent scattering of a Gaussian wave packet with a negative statistical correlation between the particle's position and momentum. Our results confirm that wave packet contraction is indeed possible before and after the barrier scattering, which opens the possibility of more precise position measurements with this type of potential.

METHODS

Step Potential Barrier

The step potential barrier problem consists of a particle that is free to move everywhere up to a certain point. Beyond this point, the particle encounters a potential that increases sharply (Zettili 2009). If the origin is the critical point, we define the step barrier as:

$$V(x) = \begin{cases} 0, x < 0 \\ V_0, x \geq 0 \end{cases} \quad (1)$$

for some constant value $V_0 > 0$. Consider a particle of mass m and kinetic energy E, incident in the positive x direction, and initially localized in Region I ($x < 0$). At $x = 0$, the particle experiences a repulsive potential.

Suppose $E > V_0$. In classical mechanics, when a particle with constant momentum $p_1 = \sqrt{2mE}$ encounters the barrier, it will be transmitted through Region II ($x > 0$). It slows down with momentum $p_2 = \sqrt{2m(E - V_0)} < p_1$ and the transmitted particle has a smaller kinetic energy $E - V_0$. Note that the particle is influenced by a force only at the origin. The particle is free in Regions I and II since the potentials are constant there. If we consider $E < V_0$ instead, then according to classical mechanics, no transmission is possible, and the particle is reflected back. Region II is thus described as the classically forbidden region.

Quantum mechanically, this situation is typically described by the plane-wave and evanescent solutions of the TISE, representing particles with definite momentum (Griffiths 2005; Sakurai and Napolitano 2020). If $E > V_0$, a particle approaching a barrier may be either reflected or transmitted, and each outcome is associated with a probability expressed in terms of the transmission and reflection coefficients (Galiffi 2015). Even though the particle has sufficient kinetic energy to pass through Region II, the reflection coefficient may be non-zero. The particle can be reflected by the barrier despite the fact that $E > V_0$, in contrast to the classical case. A transmission coefficient approaches unity (which corresponds to a 100% probability of transmission into Region II) whenever $E \gg V_0$. For $E < V_0$ the evanescent solution in the classically forbidden region implies that the particle has a non-zero probability of being found within the barrier region.

An interesting situation occurs when the particle is not in a state of definite momentum and is, thus, represented by a wave packet. Dai *et al.* (2005) simulated the scattering event of a Gaussian wave packet hitting a step potential barrier using the finite difference time domain method to solve the TDSE. The wave packet has energy $E = 146$ eV and $V_0 = 100$ eV, and as expected from the literature, the original wave packet split into two wave groups – a reflected wave and a transmitted wave. This non-classical effect is analogous to the Schrödinger cat paradox, where the cat is in a superposition state of being "alive" and "dead." Like the cat, the scattering particle is in a superposition state of being "reflected" and "transmitted." Of course, if we perform a position measurement, then according to the von Neumann projection postulate the separated wave packets will instantaneously collapse, destroying the superposition state. We then know if the particle has been reflected or transmitted if it is found in Region I or II, respectively.

Crank-Nicolson (C-N) Algorithm

The C-N numerical scheme is a standard technique for solving partial differential equations through the finite difference forms of the space and time derivatives. The C-N method is a combination of implicit and explicit methods that is unconditionally stable (Hjorth-Jensen 2015). Purwaningsih and Fardela (2022) solved the TDSE equation using the C-N method in the MATLAB programming language. They simulated the time evolution of the dispersive free-space Gaussian wave packet and showed that the C-N method conserves the norm of the wave packet and is second-order accurate in time. Khan *et al.* (2022) showed that the C-N method when applied to the TDSE is unconditionally stable and accurate without any restrictions on the time step and spatial interval spacing.

The first step to solve the TDSE is to discretize the problem by defining a two-dimensional spatial grid of N points in both x and t axes. It is convenient to solve the problem in Hartree atomic units, where $\hbar = 1$ (Drake 2006). At each point (x, t) on the grid, the x and t components are defined mathematically as:

$$x = j \cdot h_x \tag{2}$$
$$t = n \cdot h_t \tag{3}$$

where j and n are both integer indices that take a value that is greater than or equal to zero ($j, n = 0, 1, 2, 3, \ldots, N-1$), and h_x and h_t correspond to the spacing between two points of the grid axes. We denote the wave function Ψ and potential V at a given point in space x_j and time $t_n = t_0 + nh_t$ as:

$$\Psi(x_j, t_n) = \Psi_j^n \tag{4}$$
$$V(x_j) = V_j \tag{5}$$

respectively, where t_0 is the initial time. In this discretized space, the partial derivatives of the wave function $\Psi(x,t)$ can be approximated by the forward time centered space (FCTS) approximation using the forward difference approximation:

$$\frac{\partial \Psi}{\partial t} = \frac{\Psi_j^{n+1} - \Psi_j^n}{h_t} \tag{6}$$

$$\frac{\partial \Psi}{\partial x} = \frac{\Psi_{j+1}^n - \Psi_j^n}{h_x} \tag{7}$$

with error terms of order $(h_t)^2$ and $(h_x)^2$, respectively. The second partial derivative in x is:

$$\frac{\partial^2 \Psi}{\partial x^2} = \frac{\Psi_{j+1}^n - 2\Psi_j^n + \Psi_{j-1}^n}{{h_x}^2} \tag{8}$$

Hence, the discretized TDSE is:

$$i\frac{\Psi_j^{n+1} - \Psi_j^n}{h_t} = -\frac{1}{2m}\frac{\Psi_{j+1}^n - 2\Psi_j^n + \Psi_{j-1}^n}{{h_x}^2} + V_j\Psi_j^n \tag{9}$$

where $i = \sqrt{-1}$ and m is the particle's mass. An alternate approximation to the TDSE is the backward time centered space (BTCS) approximation, where the spatial derivatives are evaluated at the $n+1$ time step, thus:

$$i\frac{\Psi_j^{n+1} - \Psi_j^n}{h_t} = -\frac{1}{2m}\frac{\Psi_{j+1}^{n+1} - 2\Psi_j^{n+1} + \Psi_{j-1}^{n+1}}{{h_x}^2} + V_j\Psi_j^{n+1} \tag{10}$$

Unfortunately, both FTCS and BTCS discretization schemes are not simultaneously stable and unitary. These drawbacks are eliminated in the C-N method, which takes the average of Equations 9 and 10, which obtains:

$$i\frac{\Psi_j^{n+1} - \Psi_j^n}{h_t} = \frac{1}{4m}\left(-\frac{\Psi_{j+1}^n - 2\Psi_j^n + \Psi_{j-1}^n}{{h_x}^2} - \frac{\Psi_{j+1}^{n+1} - 2\Psi_j^{n+1} + \Psi_{j-1}^{n+1}}{{h_x}^2}\right) + \frac{1}{2}\left(V_j\Psi_j^n + V_j\Psi_j^{n+1}\right) \tag{11}$$

This difference equation is [a] implicit, [b] symmetric in time, and [c] second-order accurate in time. If we perform a von Neumann stability analysis, the amplification factor is:

$$\xi = \frac{1 - \frac{ih_t}{2}\left(\frac{2}{{h_x}^2}\left(\sin\frac{kh_x}{2}\right)^2 + V_j\right)}{1 + \frac{ih_t}{2}\left(\frac{2}{{h_x}^2}\left(\sin\frac{kh_x}{2}\right)^2 + V_j\right)} \tag{12}$$

where k is a real valued wave number (Press et al. 1986). By inspection, for any choice of h_t and h_x, we have $|\xi|^2 < 1$; hence, the C-N method is numerically stable. Using some algebra, the C-N difference equation can be rearranged, and we obtain:

$$\left(-i + 2\mu + \frac{h_t}{2}V_j\right)\Psi_j^{n+1} - \mu\Psi_{j+1}^{n+1} - \mu\Psi_{j-1}^{n+1} = -\left(i + 2\mu + \frac{h_t}{2}V_j\right)\Psi_j^n + \mu\Psi_{j+1}^n + \mu\Psi_{j-1}^n \tag{13}$$

where:

$$\mu = \frac{h_t}{4(h_x)^2} \tag{14}$$

This gives us the wave function at time step $n+1$ on the LHS and the wave function at time step n at the RHS. Finally, if we define:

$$W_j = 2\mu + \frac{h_t}{2}V_j \tag{15}$$

we can rewrite the difference equation as:

$$-\mu\Psi_{j-1}^{n+1} + (W_j - i)\Psi_j^{n+1} - \mu\Psi_{j+1}^{n+1} = \mu\Psi_{j-1}^n - (W_j + i)\Psi_j^n + \mu\Psi_{j+1}^n \tag{16}$$

for $j = 2, 3 \ldots N-1$, which can be expressed as the matrix equation:

$$\begin{bmatrix} W_1 - i & -\mu & 0 & & 0 \\ -\mu & W_2 - i & -\mu & \cdots & 0 \\ 0 & -\mu & W_3 - i & & 0 \\ & \vdots & & \ddots & \vdots \\ 0 & 0 & 0 & & 0 \\ 0 & 0 & 0 & \cdots & -\mu \\ 0 & 0 & 0 & & W_3 - i \end{bmatrix} \begin{bmatrix} \Psi_1^{n+1} \\ \Psi_2^{n+1} \\ \Psi_3^{n+1} \\ \vdots \\ \Psi_{N-3}^{n+1} \\ \Psi_{N-2}^{n+1} \\ \Psi_{N-1}^{n+1} \end{bmatrix}$$
$$= \begin{bmatrix} -(W_1 + i) & \mu & 0 & & 0 \\ \mu & -(W_2 + i) & \mu & \cdots & 0 \\ 0 & \mu & -(W_3 + i) & & 0 \\ & \vdots & & \ddots & \vdots \\ 0 & 0 & 0 & & 0 \\ 0 & 0 & 0 & \cdots & \mu \\ 0 & 0 & 0 & & -(W_{N-1} + i) \end{bmatrix} \begin{bmatrix} \Psi_1^n \\ \Psi_2^n \\ \Psi_3^n \\ \vdots \\ \Psi_{N-3}^n \\ \Psi_{N-2}^n \\ \Psi_{N-1}^n \end{bmatrix} \tag{17}$$

The column matrix on the right-hand side of Equation 17 represents the wave function Ψ at time step n. Initializing the wave function Ψ_j^0 at time step $n = 0$ allows us to solve the wave function at the next time step Ψ_j^1 using Equation 16, which in turn permits us to solve for Ψ_j^2 and so on for subsequent time steps.

The form of the amplification factor from the von Neumann analysis result suggests that the C-N method is stable for any choice of h_t and h_x. To ensure its robustness in performing accurate numerical calculations

of this approach, we tested the algorithm. As the barrier height increased while keeping the initial energy fixed, the transmission and reflection coefficients approached 0 and 1, respectively. Additionally, the opposite limit was reached as the barrier height approached zero. The expected outcomes in the simulation were achieved and no unphysical results were found.

Table 1 depicts the percent difference between the analytical and numerical value for the position expectation value $\langle x \rangle$ and the position uncertainty Δx of the Gaussian wave packet for comparison. Based on the data for the percent error, the values obtained numerically by the C-N method admit analytical results.

Table 1. Position uncertainty and position expectation value (in Hartree atomic units) of the squeezed Gaussian wave packet using the C-N method (as shown in Figures 1 and 2) *vs.* time *via* the numerical quadrature (trapezoidal). The analytic results from Equations 24) and (25) and the percentage error of the numerical integration are included for comparison.

	Time	Analytic	C-N scheme	Percent difference
$\langle x \rangle$	$t = 4.00$	12.0	11.99	0.0667%
	$t = 8.00$	28.0	28.0	0.0571%
	$t = 12.00$	44.0	44.0	0.0545%
	$t = 16.00$	60.0	60.0	0.0533%
	$t = 20.00$	76.0	76.0	0.0526%
Δx	$t = 4.00$	2.00	2.00	0.1110%
	$t = 8.00$	1.41	1.41	0.0017%
	$t = 12.00$	2.00	1.99	0.3470%
	$t = 16.00$	3.16	3.15	0.3720%
	$t = 20.00$	4.47	4.46	0.3520%

Squeezed Gaussian Wave Packet

Robinett and co-workers (2005) examined a Gaussian wave packet in position space with an initial non-zero statistical correlation between the position and momentum, given by:

$$\Psi(x,t) = A(t)\exp\left(ip_0(x-x_0)\right)\exp\left(-\frac{ip_0^2}{2m}t\right)\exp\left(-\frac{(x-x_0-p_0t/m)^2}{2\beta^2(1+i(C+t/t_0))}\right) \quad (18)$$

in Hartree atomic units, where $\hbar = 1$ (Teo and Li 2011; Drake 2006), where:

[a] m is the particle's mass, and x_0 and p_0 are the arbitrary initial position and momentum expectation values of this state at time $t = 0$;

[b] β is a positive real-valued parameter with dimensions of length that sets the initial momentum uncertainty $(\Delta p)_0$, where:

$$(\Delta p)_0 = \frac{1}{\beta\sqrt{2}} \quad (19)$$

[c] C is a real-valued dimensionless parameter (referred to as the correlation parameter) proportional to the initial value of the statistical correlation between the position and momentum;

[d] t_0 is a positive real-valued parameter with dimensions of time (referred to as the coherence time), equal to:

$$t_0 = m\beta^2 \quad (20)$$

and [e] $A(t)$ is the complex-valued coefficient function.

$$A(t) = \frac{1}{\sqrt{\beta\left(1+i(C+t/t_0)\right)\sqrt{\pi}}} \quad (21)$$

In this paper, following Robinett et al. (2005), we refer to Equation 18 as the squeezed Gaussian wave packet. Note that setting $C = 0$ at $t = 0$ in Equation 18 recovers the usual minimum uncertainty Gaussian wave packet typically discussed in quantum mechanics textbooks:

$$\Psi(x,t) = A(t)\exp\left(ip_0(x-x_0)\right)\exp\left(-\frac{(x-x_0)^2}{2\beta^2}\right) \quad (22)$$

Recall that for a free particle, the TDSE is:

$$i\frac{\partial}{\partial t}\Psi = -\frac{1}{2m}\frac{\partial^2}{\partial x^2}\Psi \quad (23)$$

Let $\bar{x} = x_0 + p_0 t/m$ and $\epsilon = C + t/t_0$. Using Equation 18, observe that:

$$i\frac{\partial}{\partial t}\Psi = \Psi\left(\frac{1}{2m\beta^2(1+i\epsilon)} + \frac{{p_0}^2}{2m} + \frac{ip_0}{m\beta^2}\frac{(x-\bar{x})}{(1+i\epsilon)} - \frac{1}{2m\beta^4}\frac{(x-\bar{x})^2}{(1+i\epsilon)^2}\right) \quad (24)$$

$$\frac{\partial}{\partial x}\Psi = \Psi\left(ip_0 - \frac{(x-\bar{x})}{\beta^2(1+i\epsilon)}\right) \quad (25)$$

$$\frac{\partial^2}{\partial x^2}\Psi = \Psi\left(ip_0 - \frac{(x-\bar{x})}{\beta^2(1+i\epsilon)}\right)^2 - \Psi\frac{1}{\beta^2(1+i\epsilon)} \quad (26)$$

Multiplying Equation 26 by $-1/2m$, expanding it, and comparing it with Equation 24 obtains Equation 23. Hence the wave function (Equation 18) satisfies the free particle TDSE.

The corresponding position probability density is:

$$|\Psi(x,t)|^2 = \frac{1}{\beta\sqrt{\pi}\sqrt{(1+(C+t/t_0)^2)}}\exp\left(-\frac{(x-x_0-p_0t/m)^2}{\beta^2(1+(C+t/t_0)^2)}\right) \quad (27)$$

The position expectation value and position uncertainty are respectively:

$$\langle x \rangle = x_0 + \frac{p_0 t}{m} \tag{28}$$

$$\Delta x = \left((\Delta x)_0{}^2 + C\beta^2 \frac{t}{t_0} + \frac{\beta^2 t^2}{2 t_0{}^2} \right)^{1/2} = \left((\Delta x)_0{}^2 + C\frac{t}{m} + ((\Delta p)_0)^2 \frac{t^2}{m^2} \right)^{1/2} \tag{29}$$

We note two things from Equation 29. First, Equation 29 shows that the correlation parameter C is responsible for the expansion and contraction of the squeezed Gaussian wave packet through the increase or decrease of its position uncertainty Δx. If $C \geq 0$ then the position uncertainty Δx will increase monotonically over time. If $C < 0$ it is possible for $\Delta x < (\Delta x)_0$ for a certain amount of time, i.e. the position uncertainty actually decreases, and the particle is more localized. Second, the parameter t_0 effectively sets a time scale for this duration since this contraction is not possible for $t \gg t_0$. Hence, Robinett et al. (2005) identified t_0 as the coherence time of the squeezed Gaussian wave packet.

The correlation parameter C is proportional to the initial value of the statistical correlation between the position and momentum observables for a given wave packet. Recall that the statistical covariance between any two random variables X and Y is given by:

$$\mathrm{cov}(X, Y) = \langle (X - \langle X \rangle)(Y - \langle Y \rangle) \rangle \tag{30}$$

with respect to some probability distribution. In quantum mechanics where the random variables are the position and momentum operators $X \to \hat{x}$ and $Y \to \hat{p}$, we must take into account the fact that the position and momentum operators are not compatible, i.e.:

$$[\hat{x}, \hat{p}] = i \iff \hat{x}\hat{p} \neq \hat{p}\hat{x} \tag{31}$$

so that operator ordering matters. Hence, any classical product xp must be symmetrized, and it is standard practice to use the Weyl ordering (Sakurai and Napolitano 2020):

$$xp \to \frac{1}{2}(\hat{x}\hat{p} + \hat{p}\hat{x}) \tag{32}$$

and the time-dependent statistical covariance between x and p is modified to:

$$\mathrm{cov}(\hat{x}, \hat{p}) = \frac{1}{2}\langle (\hat{x} - \langle \hat{x} \rangle)(\hat{p} - \langle \hat{p} \rangle) + (\hat{p} - \langle \hat{p} \rangle)(\hat{x} - \langle \hat{x} \rangle) \rangle \tag{33}$$

evaluated with respect to the given state (Bohm 1951; Levy-Leblond 1986; Campos 1998; Robinett et al. 2005; Riahi 2013; Neto et al. 2015). In terms of the squeezed Gaussian state, the statistical covariance is (Robinett et al. 2005):

$$\kappa(t) = \mathrm{cov}(\hat{x}, \hat{p}) = \frac{1}{2}\left(C + \frac{t}{t_0} \right) \tag{34}$$

and therefore $\kappa(0) = C/2$. This implies that if the position and momentum have a negative statistical correlation $\kappa(0) < 0$ at the initial time $t = 0$, we must then necessarily have $C < 0$. By the previous argument, wave packet contraction will occur. To calculate the contraction duration, note that Equation 29 has the time rate of change:

$$r(t) = \frac{d}{dt}\Delta x = \frac{1}{2\Delta x}\frac{C\beta^2}{t_0}\left(1 + \frac{t}{C t_0} \right) \tag{35}$$

which is linear in time t. Let $t_{min} = -Ct_0$ and note that $t_{min} > 0$ since $C < 0$. This means:

$$r(t) \begin{cases} < 0 \text{ if } t < t_{min} \\ = 0 \text{ if } t = t_{min} \\ > 0 \text{ if } t > t_{min} \end{cases} \tag{36}$$

At time t_{min}, the position uncertainty is:

$$\Delta x_{min} = \left((\Delta x)_0{}^2 - \frac{C^2\beta^2}{2} \right)^{1/2} < (\Delta x)_0 \tag{37}$$

and $r(t)$ implies that is the minimum position uncertainty. At time $t = 2t_{min}$, we have $\Delta x = (\Delta x)_0$. For $t > t_{min}$, the position uncertainty increases monotonically. Hence, the wave packet contraction occurs within the time interval $0 \leq t \leq 2t_{min}$. The time rate of change of the position uncertainty and the statistical covariance are proportional at any time t:

$$r(t) = \frac{d}{dt}\Delta x = \frac{1}{\Delta x}\frac{\beta^2}{t_0}\mathrm{cov}(\hat{x}, \hat{p}) \tag{38}$$

Hence, a negative statistical correlation between position and momentum implies wave packet contraction, a positive correlation implies wave packet spreading, and a vanishing correlation implies the minimum position uncertainty.

Figure 1 illustrates the previous discussion. It shows the time evolution of a squeezed Gaussian wave packet in free space using the C-N scheme. The authors used the following parameter values in Hartree atomic units, where $\hbar = 1$ (Teo and Li 2011; Drake 2006):

- mass $m = 1.00$ atomic units (au),
- $\beta = 2.00$ au,
- correlation parameter $C = -2.00$,
- initial position expectation value $x_0 = -4.00$ au

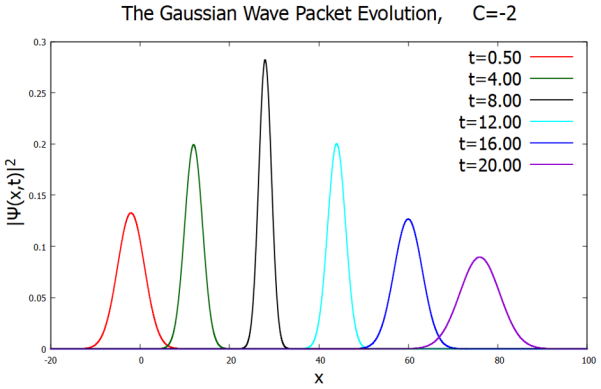

Figure 1. The time evolution of squeezed Gaussian wave packet in free space using the Crank-Nicolson scheme with the following parameter values (in Hartree atomic units): mass $m = 1.00$ au, $\beta = 2.00$ au, correlation parameter $C = -2.00$, initial position expectation value $x_0 = -4.00$ au, and initial momentum expectation value $p_0 = 4.00$ au.

- initial position uncertainty $(\Delta x)_0 = 3.16$ au
- initial momentum expectation value $p_0 = 4.00$ au.

which results in:

- a coherence time of $t_0 = 4.00$ au,
- an initial negative statistical correlation $\mathrm{cov}(\hat{x},\hat{p}) = -1$,
- $t_{min} = 8.00$ au, and
- $\Delta x_{min} = 1.41$ au.

Note that a mass of 1 au is equivalent to the electron mass and a length of 1 au corresponds to the Bohr radius (Drake 2006). The minimum position uncertainty occurs at $t = 8.00$ au and the duration of the contraction is 16.00 au. The physical interpretation of negative statistical correlation, as well as its duration and limitation, are discussed originally by Robinett *et al.* (2005) and Villanueva (2018). The squeezed Gaussian state is not unique; there is an entire class of free particle states that exhibit wave packet contraction if $C < 0$ (Villanueva 2018). A position-measurement scheme is discussed by Storey *et al.* (1994), which prepares an atom in such a contractive state.

A specific value of the correlation parameter C can be associated with an initial time t_0, as well as initial expectation values x_0 and p_0 for position and momentum respectively. For example, suppose:

- For $\Psi_A = \Psi(x, t_0)$ we have $C = 0$, $t = t_0$, $\langle\hat{x}(t_0)\rangle = x_0$ and $\langle\hat{p}(t_0)\rangle = p_0$
- For $\Psi_B = \Psi(x, t_B)$ we have $C = C_B$, $t = t_B$, $\langle\hat{x}(t_B)\rangle = x_B$ and $\langle\hat{p}(t_B)\rangle = p_B$

where Ψ is the squeezed Gaussian wave packet Equation 18.

Under what conditions can we say that the wave functions Ψ_A and Ψ_B represent the same physical state? Keeping in mind that the TDSE is not Lorentz invariant but rather Galilean invariant (Hamermesh 1960), we can imagine that Ψ_A is defined in one coordinate system A and Ψ_B in another coordinate system B, where the coordinates are of necessity related by the translation equations:

$$t_B = T + t_0 \tag{39}$$

$$x_B = X + x_0 \tag{40}$$

$$\frac{p_B}{m} = V + \frac{p_0}{m} \tag{41}$$

where:

- m is the invariant particle mass,
- T is the difference in the (absolute) time between inertial frames A and B,
- X is the spatial distance between the origins of frames A and B at the initial time, and
- V is the relative velocity between the frames A and B.

Hence, when confronted by a non-zero correlation coefficient C_B, we are at liberty to "slide" to another inertial frame where $C = 0$, provided the new frame is related to the old frame by the translation equations above.

Standard Quantum Limit

The position uncertainty imposes a fundamental limit on how accurately we can measure the position of an object. In this discussion, we recall that the object's momentum uncertainty also contributes to this uncertainty, and this dynamically induced noise in the position measurement of a free mass is referred to in the literature as the standard quantum limit or SQL (Yuen 1983; Braginsky and Khalili 1992; Giovannetti et al. 2004).

The investigation of contractive states was initiated by Yuen (1983). He was motivated by the possible enhancement of gravitational wave detection if the SQL could somehow be overcome. The position of a test mass (which will react as a gravitational wave passes it by) must be accurately and continuously monitored (Caves et al. 1980). The SQL arises in this context by directly applying the Heisenberg relation to two consecutive measurements of the position of the test mass. Suppose that we perform the first position measurement at time $t = 0$ with an uncertainty $(\Delta x)_0$. This corresponds (via the Heisenberg uncertainty relation) to an uncertainty in the initial momentum p at least equal to $(\Delta p)_0 = 1/2(\Delta x)_0$.

If the test mass is free and the initial position-momentum correlation is zero, then the uncertainty in the initial momentum $(\Delta p)_0$ transfers into an uncertainty in the position via:

$$(\Delta x)^2 = (\Delta x)_0{}^2 + ((\Delta p)_0)^2 \frac{t^2}{m^2} \tag{42}$$

This is the SQL. A second position measurement at time $t > 0$ is necessarily less accurate than the first measurement. Note that for any real quantities x and y:

$$(x - y)^2 = x^2 - 2xy + y^2 \geq 0 \tag{43}$$

which implies the inequality:

$$x^2 + y^2 \geq 2xy \tag{44}$$

Hence, the SQL can also be expressed as the inequality:

$$(\Delta x)^2 \geq 2(\Delta x)_0(\Delta p)_0 \frac{t}{m} \tag{45}$$

and the minimum value of $(\Delta x)^2$ for any second position measurement must increase linearly over time. However, there is an implicit assumption that the uncertainty Δx cannot be decreased by the correlations between the position and the momentum that build up during the unitary evolution after the first measurement. However, this is the case when C is negative and, hence, the measurement limitations of the SQL can be overcome.

RESULTS AND DISCUSSION

We consider the scattering of an incident-squeezed Gaussian wave packet (representing an electron), where E at the initial time $t = 0$is equal to the barrier height of 100 eV. The free region (Region I) is the interval -100 au $\leq x \leq 0$ au, and the step barrier occupies the interval 0 au $\leq x \leq 100$ au (Region II). The chosen parameters are in Table 2 (in both Hartree atomic units and SI units), such that the entire wave packet is essentially localized in the spatial interval -100 au $\leq x \leq 0$ au within the time duration 0 au $\leq t \leq 35$ au. The initial central position of the squeezed Gaussian wave packet is at $x_0 = 45.0$ au with an initial average momentum of $p_0 = 2.71$ au.

For $C = -5$, the incident squeezed Gaussian wave packet contracted before hitting the potential barrier. The most significant interaction occurred in the approximate time interval 8 au $\leq t \leq 22$ au, which is characterized by a highly oscillatory wave packet localized around the origin. After time $t > 22$ au, the incident wave packet split into two discernable spatially separated wave groups – a reflected wave packet and a transmitted wave packet. The transmitted wave packet penetrated Region II (the barrier region), and the rest of the original wave packet was reflected back to Region I. The reflected wave packet propagated in the negative x direction while also contracting over time. The transmitted wave packet dispersed as it moved in the positive x direction in Region II. Figures 2 and 3 show snapshots of the time evolution of the wave packet before and after scattering with the barrier potential at times $t = 12.0$ au and $t = 23.5$ au, respectively. To quantify barrier reflection and transmission, the authors numerically computed the reflection and transmission probability, respectively, given by:

Table 2. The model parameters in Hartree atomic units in the case where the initial average kinetic energy of the squeezed Gaussian wave packet is equal to the barrier potential height. The corresponding SI equivalents (in MKS units) are also included for comparison.

Parameter	Physical significance	Value (in au)	Value (in MKS)
m	Mass of electron	1.00	$9.11 \times 10^{-31}\ kg$
$\hbar$	Reduced Planck constant	1.00	$1.05 \times 10^{-34}\ J.s$
x_0	Initial central position	-40.0	$2.12 \times 10^{-9}\ m$
p_0	Initial momentum	2.71	$5.40 \times 10^{-24}\ \frac{kg \cdot m}{s}$
β	$\sqrt{2(\Delta x_0)^2}$	2.67	$1.41 \times 10^{-10}\ m$
V_0	Height of the barrier	3.67	$100\ eV$
E	Kinetic energy	3.67	$100\ eV$

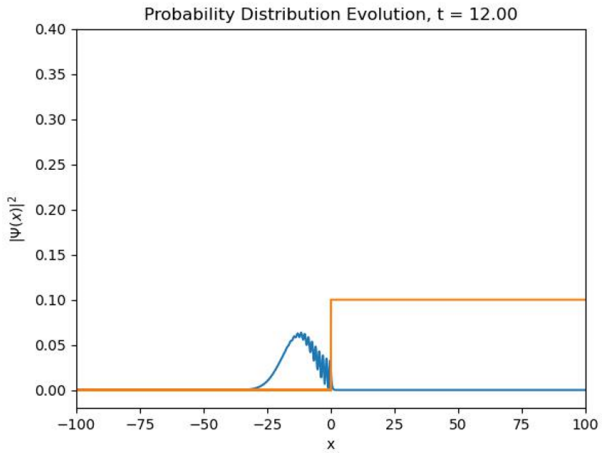

Figure 2. The position density $|\Psi(x,t)|^2|$ at time $t = 12.0$ au.

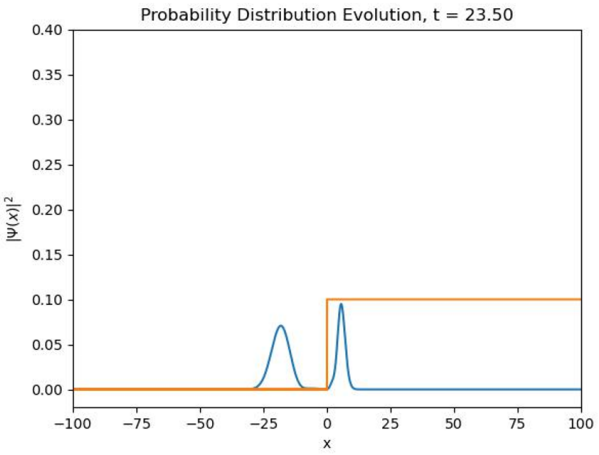

Figure 3. The position density $|\Psi(x,t)|^2|$ at time $t = 23.5$ au.

$$R = \int_{x=-100\text{ au}}^{x=0\text{ au}} |\Psi(x,t)|^2\, dx \tag{46}$$

$$T = \int_{x=0\text{ au}}^{x=100\text{ au}} |\Psi(x,t)|^2\, dx \tag{47}$$

at time $t > 22$ au when the separation between the reflected and transmitted wave packets is readily identifiable. The authors obtained $T = 0.360$ and $R = 0.640$, which imply a 36% probability of transmission into the step barrier region and a complementary probability of 64% for reflection.

When the reflected and transmitted wave packets separate after time $t > 22$ au, they are essentially free as there is negligible position amplitude at the origin for both wave packets. The incident-squeezed Gaussian wave packet prior to the scattering at time $t < 8$ au is also essentially free. Hence, the time dependence of the group velocity of these wave packets is linear in time. The C-N solution of the TDSE can be used to calculate the average position of the split wave packets after time $t > 22$ au . We solve for the position expectation values $\langle x(t)\rangle_R$ and $\langle x(t)\rangle_T$ at time t of the normalized reflected and transmitted wave packets, respectively, by numerically integrating:

$$\langle x(t)\rangle_R = \frac{1}{R}\int_{x=-100\text{ au}}^{x=0\text{ au}} x\,|\Psi(x,t)|^2\, dx \tag{48}$$

$$\langle x(t)\rangle_T = \frac{1}{T}\int_{x=0\text{ au}}^{x=100\text{ au}} x\,|\Psi(x,t)|^2\, dx \tag{49}$$

The position expectation value of the incident wave packet can be similarly computed prior to the scattering at time $t > 8$ au. We then obtain an expression for the group velocity of the transmitted and reflected wave packets by applying linear regression analysis on the position expectation data. Thus, the transmitted and reflected wave packets are moving at $\langle v\rangle_T = 1.11$ au and $\langle v\rangle_R = -2.56$ au respectively from the linear regression equations $\langle x\rangle_T = 1.11t - 20.4$ and $\langle x\rangle_R = -2.56 + 42.0$ at time $t > 22$ au.

The second moments of the position with respect to the reflected and transmitted wave packets are similarly computed from:

$$\langle x^2(t)\rangle_R = \frac{1}{R}\int_{x=-100\text{ au}}^{x=0\text{ au}} x^2\,|\Psi(x,t)|^2\, dx \tag{50}$$

$$\langle x^2(t)\rangle_T = \frac{1}{T}\int_{x=0\text{ au}}^{x=100\text{ au}} x^2\,|\Psi(x,t)|^2\, dx \tag{51}$$

which leads to the numerical values of the position uncertainty:

$$(\Delta x)_R = \sqrt{\langle x^2(t)\rangle_R - (\langle x(t)\rangle_R)^2} \tag{52}$$

$$(\Delta x)_T = \sqrt{\langle x^2(t)\rangle_T - (\langle x(t)\rangle_T)^2} \tag{53}$$

of the reflected and transmitted wave packets respectively. Figures 4 and 5 show the plots of the position uncertainty vs. time before ($t < 8$ au) and after scattering ($t > 22$ au). For $t < 8$ au, the position uncertainty of the incident squeezed Gaussian wave packet is dominated by the linear term $C\beta^2 t/t_0 = -5t$ compared to the quadratic term $\beta^2 t^2/2{t_0}^2 = t^2/8$ leading to contraction. For $t > 22$ au, performing a quadratic regression analysis on the position uncertainty data of the reflected and transmitted wave packets obtains:

$$((\Delta x)_R)^2 = 0.0383t^2 + 0.452t + 0.844 \tag{54}$$

$$((\Delta x)_T)^2 = 0.173t^2 - 3.93t + 23.2 \tag{55}$$

These expressions are consistent with contractive and dispersive propagation, respectively, of the reflected and transmitted wave packets. Hence, we have shown that the SQL can be overcome in the case of the incident and reflected wave packets, which is the main result of the paper. The extension of this investigation to other potentials is presently being considered for future work.

In contrast, Figures 6 and 7 show the position uncertainty before and after scattering of the minimum uncertainty wave packet ($C = 0$) where no contraction is observed and, therefore, the SQL applies. For additional comparisons, the position uncertainty of the free particle wave packet (red cross) is also included for $C = -5$ (Figures 4 and 5) where contraction is present and $C = 0$ (Figures 6 and 7) where contraction is absent.

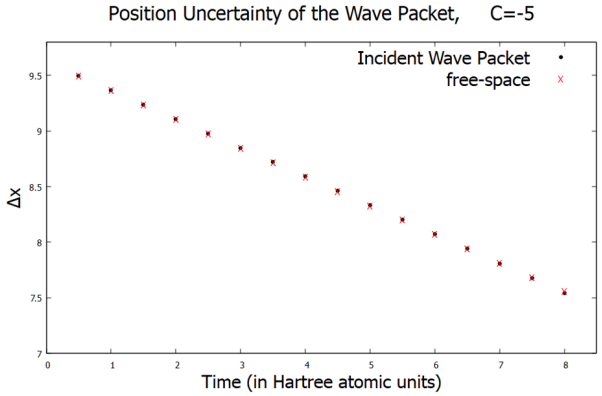

Figure 4. The position uncertainty of the squeezed Gaussian wave packet [a] incident on the step potential (black dot) and [b] of the free particle (red cross) *vs.* time t in the time interval $0 \leq t \leq 8.00$ au with $C = -5$.

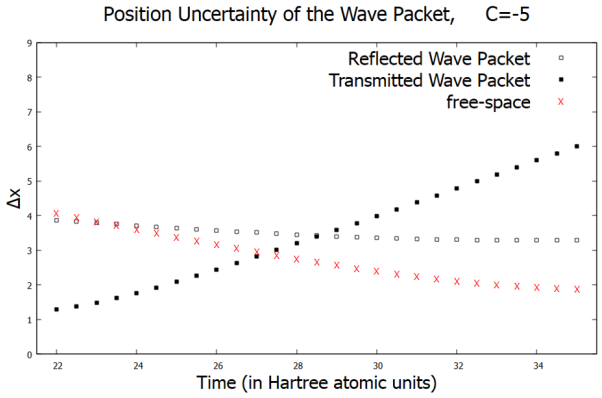

Figure 5. The position uncertainty of the [a] reflected wave packet (white dot), [b] transmitted wave packet (black dot), and [c] squeezed Gaussian wave packet of the free particle (red cross) *vs.* time t in the time interval 22 au $\leq t \leq$ 35 au with $C = -5$.

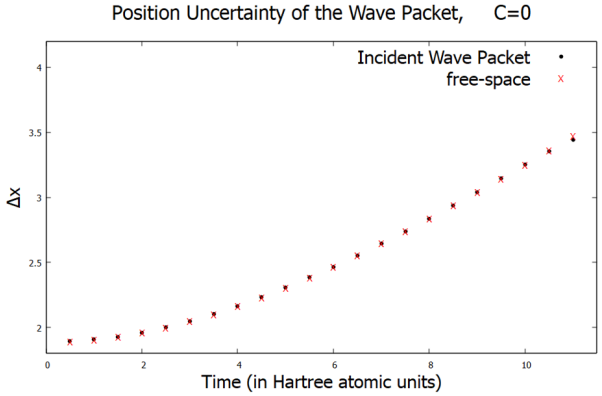

Figure 6. The position uncertainty of the squeezed Gaussian wave packet [a] incident on the step potential (black dot) and [b] of the free particle (red cross) *vs.* time t in the time interval $0 \leq t \leq 8.00$ au with $C = 0$.

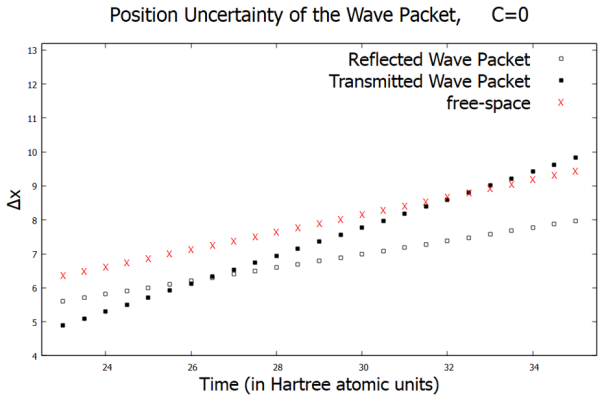

Figure 7. The position uncertainty of the [a] reflected wave packet (white dot), [b] transmitted wave packet (black dot), and [c] squeezed Gaussian wave packet of the free particle (red cross) *vs.* time t in the time interval 22 au $\leq t \leq$ 35 au with $C = 0$.

REFERENCES

BOHM D. 1951. Quantum theory. Prentice-Hall Physics Series.

BRAGINKSY VB, KHALILI FY. 1992. Quantum measurement. Cambridge University Press.

CAMPOS RA. 1998. Correlation coefficient for incompatible observables of the quantum harmonic oscillator. American Journal of Physics 66: 712–718.

CAVES CM, THORNE KS, DREVER R, SANDBERG VD, ZIMMERMANN M. 1980. On the measurement of a weak classical force coupled to a quantum-mechanical oscillator; I. issues of principle. Reviews of Modern Physics 52: 341.

DAI W, LI G, NASSAR R, SU S. 2005. On the stability of the FDTD method for solving a time-dependent Schrödinger equation. John Wiley & Sons 21(6): 1140–1154.

DRAKE GW. 2006. Springer handbook of atomic, molecular, and optical physics. Springer Science & Business Media.

GALIFFI E. 2015. Quantum reflection in two dimensions [doctorate dissertation]. Imperial College London–Universität Heidelberg.

GIOVANNETTI V, LLOYD S, MACCONE L. 2004. Quantum-enhanced measurements: beating the standard quantum limit. Science 306: 1330–1336.

GOLDBERG H, SCHEY M, SCHWARZ J. 1967. Computer-generated motion pictures of one-dimensional quantum-mechanical transmission and reflection phenomena. American Journal of Physics 35: 177–186.

GRIFFITHS D. 2005. Introduction to quantum mechanics, Pearson Prentice Hall.

HAMERMESH M. 1960. Galilean invariance and the Schrodinger equation. Annals of Physics, Vol. 9.

HJORTH-JENSEN M. 2015. Computational physics. Lecture notes, Fall 2015.

KHAN A, AHSAN M, BONYAH E, JAN R, NISAR M, ABDEL-ATY AH, YAHIA IS. 2022. Numerical solution of Schrödinger equation by Crank-Nicolson method. John Wiley & Sons 1: 6991067.

LANDAU R, PAEZ M, BORDEIANU C. 2015. Computational physics: problem solving with Python. John Wiley & Sons.

LEVY-LEBLOND JM. 1986. Correlation of quantum properties and the generalized Heisenberg inequality. American Journal of Physics 54: 135–136.

NETO, JSM, CABRAL LA, PAZ IG. 2015. Position-momentum correlations in matter waves double-slit experiment. European Journal of Physics 36(3).

PRESS W, VETTERLING W, TEUKOLSKY S, FLANNERY BP. 1986. Numerical recipes. Cambridge University Press.

PURWANINGSIH S, FARDELA R. 2022. The analysis of the physical quantity n grid, v, and dt in solving the Schrödinger equation using the Crank-Nicolson method. Jurnal Penelitian Fisika dan Aplikasinya 12(1): 1–13.

RIAHI N. 2013. The position-momentum correlation for quantum and classical probability distributions. European Journal of Physics 34(2): 461–474.

ROBINETT R, DONCHESKI M, BASSETT L. 2005. Simple examples of position-momentum correlated Gaussian free-particle wave packets in one dimension with the general form of the time-dependent spread in position. Foundations of Physics Letters 18: 455–475.

SAKURAI J, NAPOLITANO J. 2020. Modern quantum mechanics. Cambridge University Press.

SMITH K, BLAYLOCK G. 2017. Simulations in quantum tunneling. American Journal of Physics 85: 763–768.

STOREY P, SLEATOR T, COLLETT M, WALLIS D. 1994. Contractive states of a free atom. Physical Review A 49: 2322–2328.

TANNOR D. 2007. Introduction to quantum mechanics: a time-dependent perspective. University Science Books.

TEO BK, LI WK. 2011. The scales of time, length, mass, energy, and other fundamental physical quantities in the atomic world and the use of atomic units in quantum mechanical calculations. Journal of Chemical Education 88: 921–928.

VAN DIJK W, SPRUNG D, CASTONGUAY-PAGE Y. 2020. Tunnelling of Hermite-Gaussian wavepackets. Physica Scripta 95.6: 065223.

VILLANUEVA AAD. 2018. Self-focusing quantum states. American Journal of Physics 86: 126–134.

YUEN HP. 1983. Contractive states and the standard quantum limit for monitoring free-mass positions. Physical Review Letters 51: 719.

ZETTILI N. 2009. Quantum mechanics, concepts, and applications. John Wiley & Sons.